

Original Article

Circular RNA circMAGI3 accelerates the glycolysis of non-small cell lung cancer through miR-515-5p/HDGF

Feng Guo, Shanqing Li, Chao Guo, Xiaohui Xu, Xiaoyun Zhou, Dongjie Ma, Zhili Cao, Zhongxing Bing, Yushang Cui

Department of Thoracic Surgery, Peking Union Medical College Hospital, Peking Union Medical College and Chinese Academy of Medical Sciences, Beijing 100730, China

Received March 15, 2020; Accepted July 3, 2020; Epub July 15, 2020; Published July 30, 2020

Abstract: The emerging roles of circular RNAs (circRNAs) in non-small cell lung cancer (NSCLC) have been convincingly proved. However, there are still numerous unknown circRNAs needing exploration. Here, present research performed a circRNA microarray analysis for the expression profile and identified a novel circRNA (circMAGI3, hsa_circ_0110498). Clinically, circMAGI3 was significantly up-regulated in NSCLC tissue and cells, which was closely correlated with unfavorable outcome for NSCLC patients. Functionally, circMAGI3 promoted the glycolysis and proliferation of NSCLC cells. Mechanistically, circMAGI3 functioned as a sponge for miR-515-5p to relieve its target gene HDGF expression, thereby accelerating the glycolysis of NSCLC. Collectively, this research identified the oncogenic role of circMAGI3 in the tumorigenesis through miR-515-5p/HDGF axis, providing a vital theoretical basis for treatment of NSCLC.

Keywords: NSCLC, circMAGI3, glycolysis, HDGF

Introduction

Non-small cell lung cancer (NSCLC) is the one of most common and major leading cause of cancer-related death worldwide [1, 2]. The prevalence rate of NSCLC is increased yearly. Specially, the metastasis occurs at early stage in NSCLC [3]. Current mainstream treatments for NSCLC are combined with surgery, chemotherapy and immunotherapy. Although great efforts were devoted, including surgical techniques and adjuvant chemotherapies, the prognosis of NSCLC remains poor [4, 5]. Therefore, it is important to explore the molecular in the malignant progression of NSCLC, and a better knowledge during the metastasis may lead to improvements for a better treatment.

The covalently closed circular RNAs (circRNAs) have been found in eukaryotic cells for decades [6]. Initially, circRNAs were misinterpreted as the by-products of splicing errors [7]. With the rapid development of high-throughput sequencing, more and more novel circRNAs were identified in multiple cancers [8]. For example,

microarray reveals the circRNA profiles in NSCLC and found that hsa_circ_0007385 acts as an oncogene in NSCLC tumorigenesis [9]. Circ-ARHGAP10 is significantly upregulated in both NSCLC tissues and cell lines and indicates a poor prognosis in NSCLC patients through regulating miR-150-5p/GLUT-1 axis [10]. CircPTPRA is significantly downregulated in NSCLC tissue and correlated with metastasis and inferior survival outcomes in NSCLC patients by sequestering miR-96-5p and upregulating RASSF8, indicating the circPTPRA/miR-96-5p/RASSF8/E-cadherin axis in NSCLC progression [11]. Although these findings suggest the potential regulation of circRNA in NSCLC, more investigation about circRNA and NSCLC is still further devoted.

In present research, we performed the circRNA microarray and detect the profile of circRNA in NSCLC tissue comparing to adjacent tissue. CircMAGI3 is a 447-bp length circRNA derived from MAGI3 gene 4-2 exon (hsa_circ_0110498, chr1: 114092136-114128218). This research found that circMAGI3 was up-regulated in

circMAGI3 accelerates the glycolysis of NSCLC

the NSCLC cells and functioned as an oncogene in the tumorigenesis through miR-515-5p/HDGF axis, providing a vital theoretical basis for treatment of NSCLC.

Materials and methods

Tissue specimens

Total of thirty NSCLC tissue specimens and their paired para-tumor tissue were recruited from NSCLC patients who underwent surgical excision at Peking Union Medical College and Chinese Academy of Medical Sciences. All these clinical tissue were diagnosed according to pathological diagnosis by two independent pathologists. The present clinical research was approved by the Institute Research Medical Ethics Committee of Peking Union Medical College and Chinese Academy of Medical Sciences Institute and written informed consents were obtained.

Cell culture and cell transformation

NSCLC cell lines (H322, H460, A549, H1299) and normal bronchial epithelial cells (NHBE) were obtained from American Type Culture Collection (ATCC, Manassas, VA, USA). Cells were cultured in Dulbecco's modified Eagle's medium (DMEM) (Invitrogen) supplemented with 10% FBS (fetal bovine serum, Gibco, Carlsbad, CA, USA), 100 IU/ml penicillin, 100 mg/ml streptomycin (Baomanbio, Shanghai, China) at a condition of 37°C with a humidified atmosphere containing 5% CO₂. shRNA targeting circMAGI3 for silencing using pLKO.1 plasmid and the overexpression plasmid were constructed (GenePharma, Shanghai, China). Human circMAGI3 cDNA was amplified and inserted into the pCD5-ciR vector (Greenseed Biotech Co, Guangzhou, China). Transfection was carried out using Lipofectamine 2000 (Invitrogen) according to the manufacturer's instructions. The transfected cells were cultured in 6-well plates added with medium. Fresh medium was replaced every 12 h. qRT-PCR was performed to confirm the transfection efficiency.

RNase R and actinomycin D treatment

The RNase R and Actinomycin D assays were carried out as previously described [12]. Total RNA (2 mg) was isolated and incubated for 30

min at 37°C with or without 5 U/mg RNase R (Epicentre Technologies, Madison, WI, USA) purified by a RNeasy MinElute Cleaning Kit (Qiagen, Valencia, CA, USA). Subsequently, the circular and linear transcripts analyzed by RT-PCR. For Actinomycin D assay, RNA was exposed to 2 mg/ml actinomycin D (Sigma, St. Louis, MO, USA) at indicated time point. Expression levels of circular and linear RNA were analyzed by using of a qRT-PCR assay.

RNA isolation and quantitative real-time PCR

RNA from lung cancer tissues and cell lines were extracted to reversely transcribe into cDNA using SuperScript First-Strand Synthesis system (Invitrogen, Carlsbad, Calif, US). Using cDNA, qRT-PCR was performed with SYBR Premix Taq (Applied Biosystems, US) on Applied Biosystems 7300. The primers were synthesized (Sangon, Shanghai, China) and the sequences were listed in the [Table S1](#). The relative expression levels of circRNA and miRNA were calculated using 2^{-ΔΔct} method normalized to beta-actin or U6.

CCK-8 assay

After transfection, A549 cells in six groups were washed twice with PBS and treated with trypsin. After centrifugation, cells were seeded into a 96-well plate (2 × 10³ cells per well) and cultured in 37°C. After 24 h, cell counting kit-8 (CCK-8) reagent (Dojindo Laboratories, Kumamoto, Japan) was added and the cells were cultured again. The optical density (OD) value was detected at 450 nm using an automatic enzyme-mark reader (Multiskan FC, Thermo Fisher Scientific, Waltham, MA, USA).

Glucose, lactate and ATP level measurements

After transfection for 48 h, the glucose uptake, lactate production and ATP level in the supernatant were respectively measured using glucose uptake colorimetric assay kit (Sigma-Aldrich, St. Louis, MO, USA), Lactic Acid assay kit (Nanjing KeyGen Biotech, Nanjing, China) and ATP assay kit (Beyotime, Beijing, China).

Extracellular acidification rate (ECAR) assay

ECAR was analyzed using the sequential administration of glucose (10 mM), oligomycin (1 mM) and 50 mM 2-deoxyglucose (50 mM)

circMAGI3 accelerates the glycolysis of NSCLC

using XF96 Bioenergetic Analyzers (Seahorse Bioscience). ECAR measurements was normalized to total protein content and reported as mpH/min for ECAR.

Subcellular fractionation location

Nuclear and cytoplasmic fractions of NSCLC cells were separated using PARIS Kit (Life Technologies, CA, USA) according to the manufacturer's instructions. GAPDH and U1 RNA levels were used as cytoplasm control or nuclear control. The relative rate of GAPDH and U1 in cytoplasm or nuclear portion was presented as the total RNA percentage.

Luciferase reporter assay

The wild type or mutant with potential miR-515-5p binding sites of circMAGI3 and HDGF mRNA were generated. These sequences were fused into the luciferase psi-CHECK-2 vector (Promega, Madison, WI, USA). 293T cells at 80% confluence were co-transfected with luciferase plasmids and miR-515-5p or control miRNA. After transfection (48 h), Firefly/Renilla luciferase activity was detected with a Dual-Luciferase Reporter Assay System (Promega).

Animal studies

All animal study has been approved by the animal institute of Peking Union Medical College and Chinese Academy of Medical Sciences. To detect the effect of circMAGI3 knockdown on NSCLC metastasis in vivo, 1×10^6 transfected NSCLC cells were injected into nude mice. After 3 weeks, the mice were sacrificed. The tumour sizes were measured and the tumour volumes were calculated: $V \text{ (mm}^3\text{)} = \text{width}^2 \text{ (mm}^2\text{)} \times \text{length (mm)}/2$.

Statistical analysis

Statistical analysis were determined by using GraphPad Prism version 6.0 (GraphPad Software, Inc., La Jolla, CA, USA) software and Statistic Package for Social Science (SPSS version 18.0) statistical software. Data were expressed as mean \pm SD. Pearson's Chi-squared Test or Student's T-test was used to analyze the statistic differences. Log-rank test was performed to calculate the survival rate of NSCLC patients. $P < 0.05$ was considered differences.

Results

Microarray revealed the high-expression of circMAGI3 in NSCLC tissue

In the NSCLC tissue and adjacent non-tumor tissue, circRNA microarray analysis revealed the circRNA profile (**Figure 1A**). CircMAGI3 (hsa_circ_0110498) was generated from the exon 4 to exon 2 with 447 bp length (**Figure 1B**). Sanger sequence analysis found that circMAGI3 was derived from the MAGI3 gene exons by back-splicing (**Figure 1C**). When administrated with Actinomycin D, RT-PCR indicated that the circular transcript of circMAGI3 was much more stable than the linear transcript of MAGI3 (**Figure 1D**). Besides, when administrated with RNase R, circular transcript circMAGI3 was much more stable than the linear transcript of MAGI3 (**Figure 1E**). In NSCLC tissue, circMAGI3 expression was significantly up-regulated as comparing to the normal samples (**Figure 1F**; **Table 1**). Survival rate analysis using Log-rank test revealed that higher circMAGI3 indicated the lower survival rate for NSCLC (**Figure 1G**). Overall, these data suggested the high-expression of circMAGI3 in NSCLC tissue.

CircMAGI3 promoted the glycolysis and proliferation of NSCLC

It has been identified that circMAGI3 was up-regulated in the NSCLC tissue, therefore, more investigation was performed to explore its function. In NSCLC cells, RT-PCR showed that circMAGI3 was significantly up-regulated in NSCLC cell lines (**Figure 2A**). The over-expression and knockdown of circMAGI3 were respectively constructed using A549 cells for the gain- or loss-of-functional experiments (**Figure 2B**). CCK-8 assay showed that circMAGI3 promoted the proliferative ability of A549 cells in vitro (**Figure 2C**). Moreover, the glucose uptake analysis, lactate production analysis and ATP analysis revealed that circMAGI3 overexpression promoted the glucose uptake level (**Figure 2D**), lactate production level (**Figure 2E**) and ATP yielding capacity (**Figure 2F**), while circMAGI3 knockdown repressed them. Extracellular acidification rate (ECAR) analysis showed that circMAGI3 overexpression promoted the glycolytic capacity of NSCLC cells, and circMAGI3 knockdown inhibited it (**Figure 2G**). Overall, these findings suggested that CircMAGI3 pro-

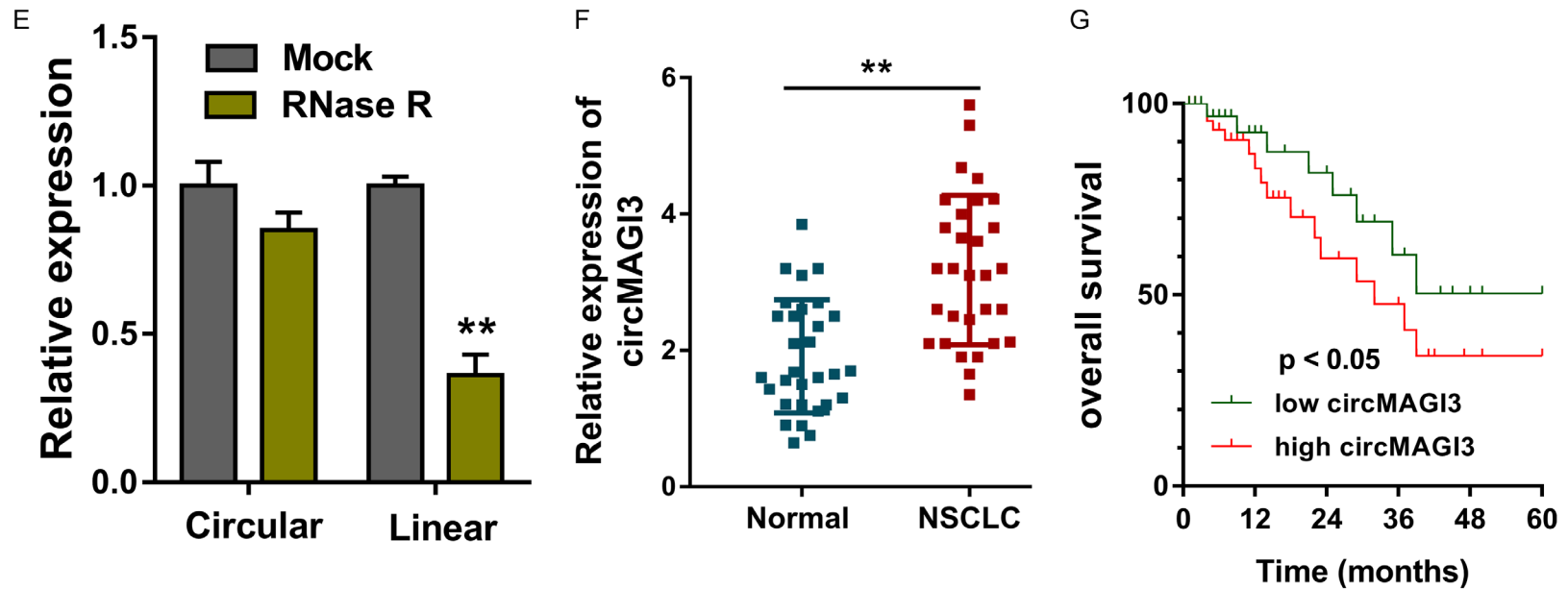


Figure 1. Microarray revealed the high-expression of circMAGI3 in NSCLC tissue. A. Heat map illustrated the circRNA microarray analysis for the circRNA profile in NSCLC tissue. B. Schematic diagram revealed that circMAGI3 (hsa_circ_0110498) was generated from the MAGI3 exons. C. Sanger sequence analysis found the conjunction sites for circMAGI3. D. RT-PCR indicated the expression of circular transcript of circMAGI3 and linear transcript of MAGI3 mRNA when administrated with Actinomycin D. E. RT-PCR indicated the expression of circular transcript of circMAGI3 and linear transcript of MAGI3 mRNA when administrated with RNase R. F. CircMAGI3 expression in NSCLC tissue as comparing to the normal samples. G. Survival rate analysis using Log-rank test revealed the survival rate for NSCLC with circMAGI3 level. **P < 0.01, data represent the means ± SD.

circMAGI3 accelerates the glycolysis of NSCLC

Table 1. Clinicopathological feature of NSCLC patients with high/low expression of circMAGI3

	Total	circMAGI3		P
		Low = 15	High = 15	
Gender				0.605
Male	18	8	10	
Female	12	7	5	
Age (years)				0.598
≥ 60	16	9	7	
< 60	14	6	8	
TNM				0.045*
I-II	11	6	5	
III/IV	19	9	10	
Lymph metastasis				0.475
No	14	6	8	
Yes	16	9	7	
Differentiation				0.208
well, moderate	15	7	8	
poor	15	8	7	

*P < 0.05 represents statistical difference.

moted the glycolysis and proliferation of NSCLC.

CircMAGI3 targeted miR-515-5p/HDGF axis

In the subcellular location analysis, data found that circMAGI3 was primarily located in the cytoplasm (**Figure 3A**). RT-PCR revealed that multiple miRNAs were dysregulated after circMAGI3 was knocked down (**Figure 3B**). Among these miRNAs, miR-515-5p was closely correlated with circMAGI3, and the wild type and mutant sequences were constructed for luciferase reporter assay (**Figure 3C**). Luciferase reporter assay found that miR-515-5p was closely connected with circMAGI3 wild type (**Figure 3D**). Online bioinformatics predictive tools found that HDGF mRNA 3'-UTR was capable of adsorbing miR-515-5p, and the wild type and mutant sequences of HDGF mRNA 3'-UTR were constructed (**Figure 3E**). Luciferase reporter assay found that miR-515-5p was closely bound with HDGF mRNA 3'-UTR (**Figure 3F**). RT-PCR showed that miR-515-5p mimics transfection repressed the HDGF mRNA expression, and miR-515-5p inhibitor transfection increased it (**Figure 3G**). Besides, circMAGI3 overexpression accelerated the HDGF mRNA expression and miR-515-5p mimics co-transfection rescued it (**Figure 3H**). Overall,

these data suggested that circMAGI3 targeted miR-515-5p/HDGF axis.

CircMAGI3/miR-515-5p/HDGF axis regulated the glycolysis and proliferation of NSCLC cells

To identify the regulation of circMAGI3/miR-515-5p/HDGF axis in NSCLC, rescue assays were performed. Results showed that miR-515-5p mimics transfection repressed the glucose uptake level (**Figure 4A**), lactate production (**Figure 4B**), ATP level (**Figure 4C**), and glycolytic capacity (**Figure 4D**) of NSCLC cells, as well as the proliferation (**Figure 4E**). Besides, the co-transfection of miR-515-5p mimics and circMAGI3 overexpression rescued the glycolysis and proliferation of NSCLC cells. Moreover, HDGF overexpression transfection promoted the glycolysis and proliferation, and the co-transfection of HDGF overexpression and circMAGI3 knockdown rescued them. In vivo xenograft

assay showed that circMAGI3 knockdown repressed the tumor volume (**Figure 4F**) and weight (**Figure 4G**) of NSCLC neoplasm. In conclusion, circMAGI3/miR-515-5p/HDGF axis regulated the glycolysis and proliferation of NSCLC cells.

Discussion

The vital roles of covalently closed circRNAs in human cancer cells have been identified in human cancer [13]. With the rapid increasing of high-throughput sequencing and bioinformatic analysis, thousands of circRNAs have been successfully discovered in multiple cancers [14]. Recently, many researchers reported numerous of circRNAs using next-generation sequencing, which were highly stable and abundantly expressed and dysregulated in diverse cancer types, such as hepatocellular carcinoma, gastric cancer, colorectal cancer, esophageal squamous cell carcinoma and so on [15].

In NSCLC samples, our research team performed the microarray analysis and found that numerous circRNAs were dysregulated in NSCLC tissue as comparing to the normal adjacent tissue [16, 17]. Among these circRNAs, circMAGI3 was significantly up-regulated in NSCLC tissue as well as the cell lines. Functional cellular experiments, gain- and loss-

circMAGI3 accelerates the glycolysis of NSCLC

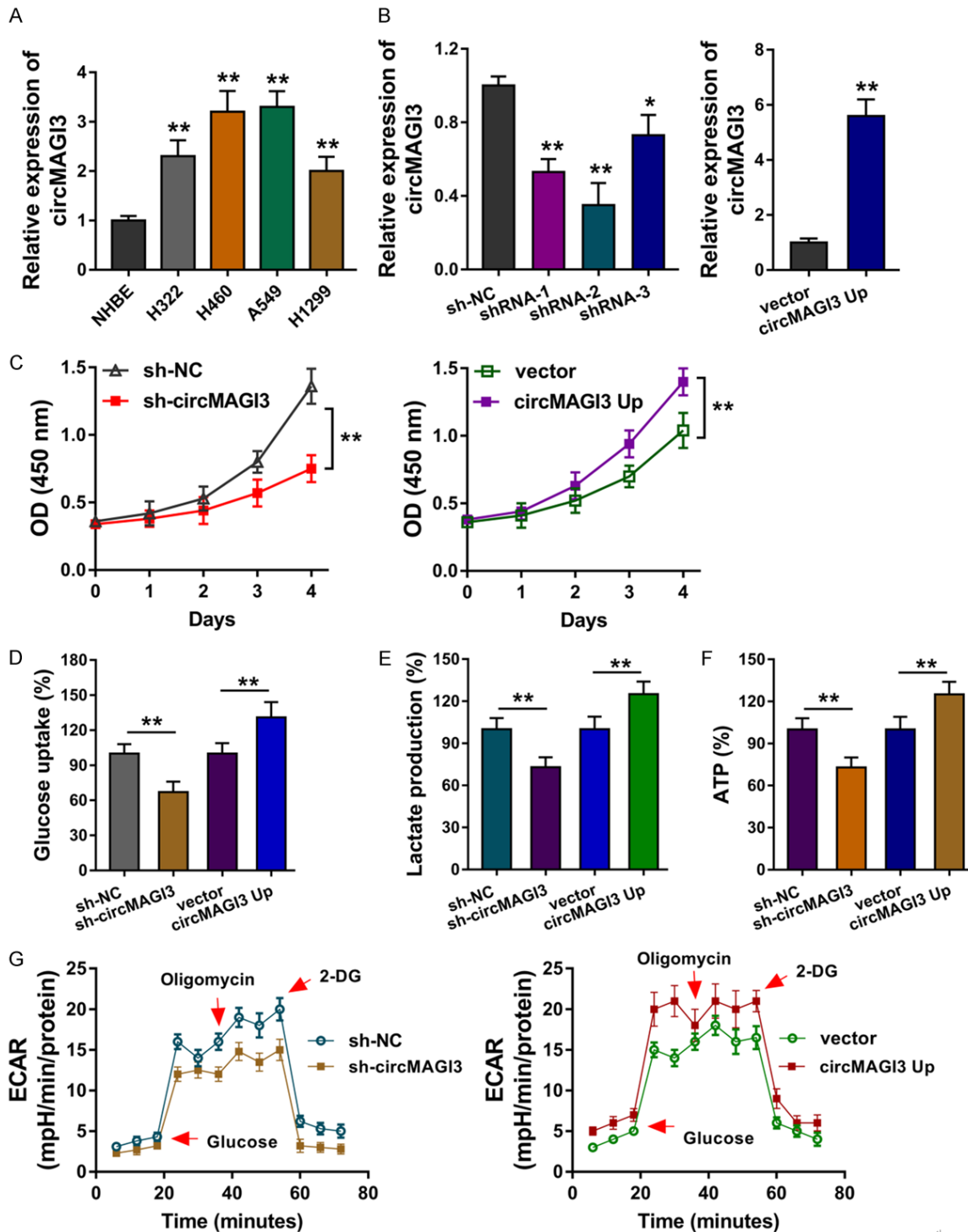


Figure 2. CircMAGI3 promoted the glycolysis and proliferation of NSCLC. (A) RT-PCR showed the circMAGI3 level in NSCLC cells and normal cells. (B) The over-expression and knockdown of circMAGI3 were respectively constructed using A549 cells for the gain- or loss-of-functional experiments. (C) CCK-8 assay showed the proliferative ability of A549 cells transfected with circMAGI3 over-expression and knockdown. (D) Glucose uptake analysis and (E) lactate production analysis and (F) ATP analysis revealed the glucose uptake level, lactate production level and ATP capacity. (G) Extracellular acidification rate (ECAR) analysis showed the glycolytic capacity of NSCLC cells. *P < 0.05, **P < 0.01, data represent the means \pm SD.

circMAGI3 accelerates the glycolysis of NSCLC

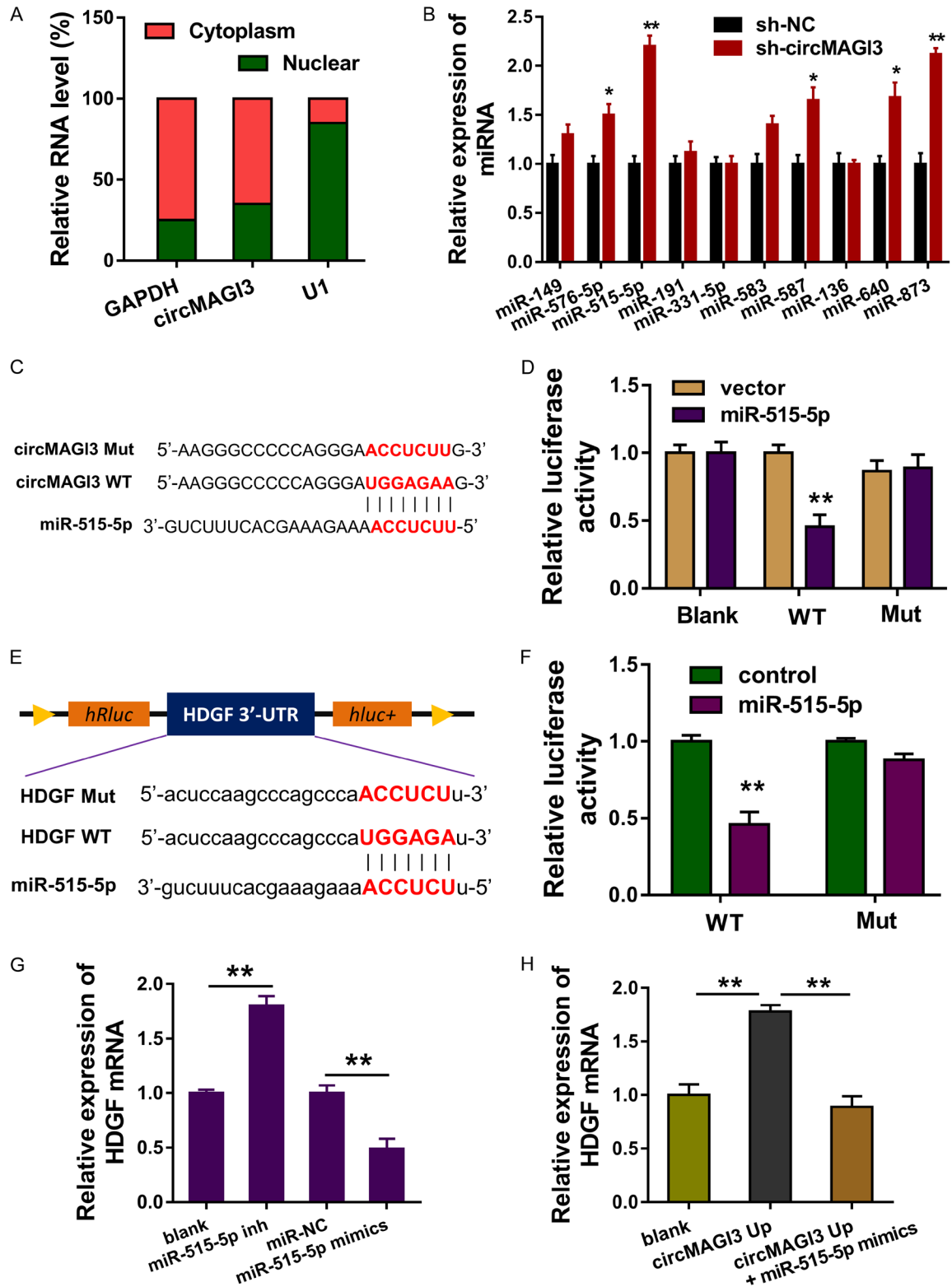


Figure 3. CircMAGI3 targeted miR-515-5p/HDGF axis. A. Subcellular location analysis illustrate the location of circMAGI3 in the cytoplasm or nuclear in NSCLC cells. B. RT-PCR revealed the expression of multiple miRNAs after circMAGI3 was knocked down. C. The wild type and mutant sequences of circMAGI3 were constructed. D. Luciferase reporter assay found the close connection of circMAGI3 wild type with miR-515-5p. E. Online bioinformatics predictive tools revealed the wild type and mutant sequences of HDGF mRNA 3'-UTR. F. Luciferase reporter assay

circMAGI3 accelerates the glycolysis of NSCLC

found the close connection of HDGF mRNA 3'-UTR wild type with miR-515-5p. G. RT-PCR showed the HDGF mRNA expression in A549 cells transfected with miR-515-5p mimics or inhibitor (inh). H. RT-PCR showed the HDGF mRNA expression in A549 cells transfected with circMAGI3 overexpression or miR-515-5p mimics. *P < 0.05, **P < 0.01, data represent the means \pm SD.

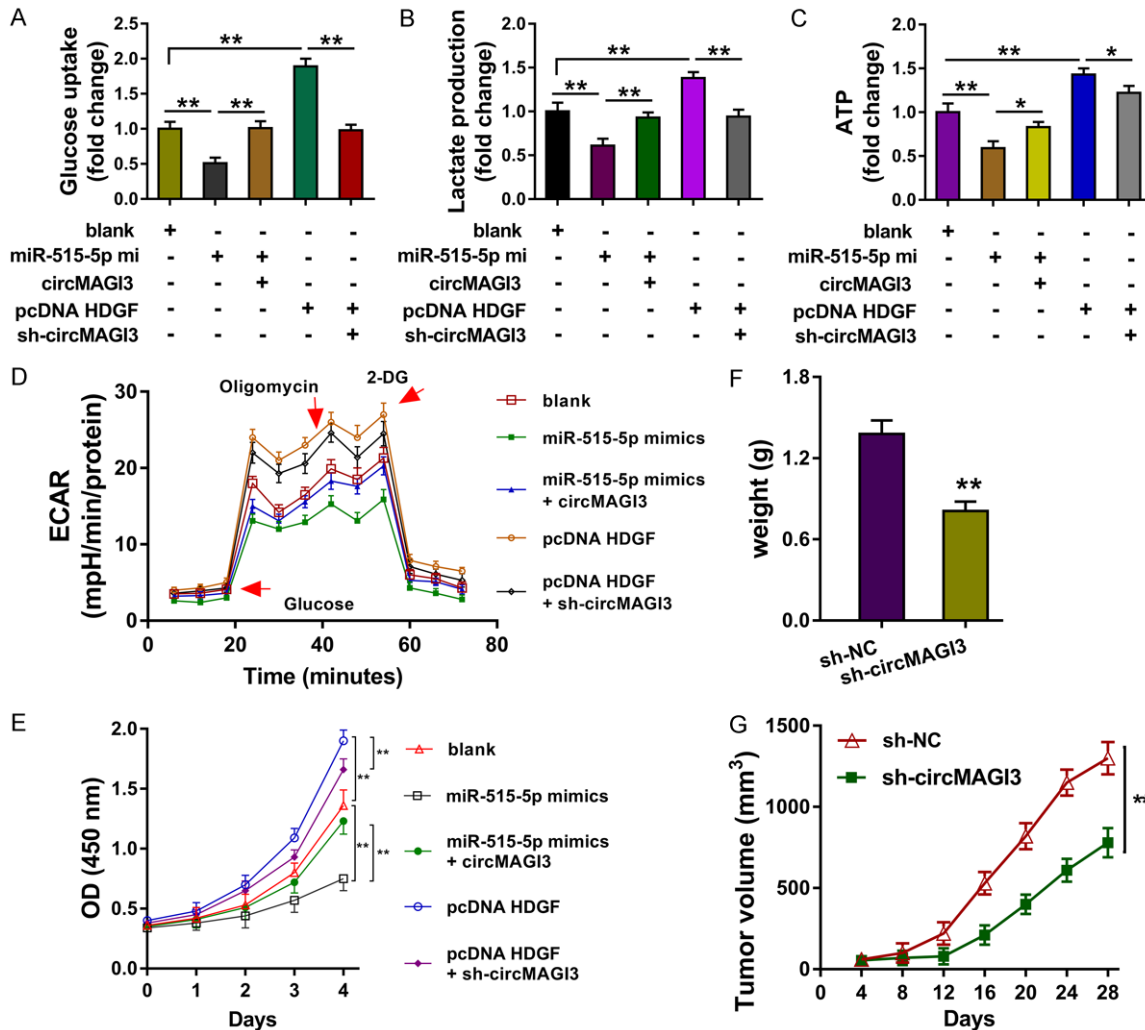


Figure 4. CircMAGI3/miR-515-5p/HDGF axis regulated the glycolysis and proliferation of NSCLC cells. (A) Glucose uptake analysis revealed the glucose uptake level in A549 cells transfected with miR-515-5p mimics, circMAGI3 overexpression, HDGF overexpression and circMAGI3 knockdown. (B) Lactate production analysis revealed the lactate level. (C) ATP analysis revealed the ATP level. (D) ECAR analysis revealed the glycolytic capacity. (E) CCK-8 revealed the proliferation. (F) The tumor volume and (G) weight of NSCLC neoplasm in mice injected with A549 cells. *P < 0.05, **P < 0.01, data represent the means \pm SD.

tional assays, found that circMAGI3 promoted the analysis and ATP analysis revealed that circMAGI3 overexpression promoted the glucose uptake level, lactate production level and ATP capacity. Extracellular acidification rate (ECAR) analysis found that circMAGI3 overexpression promoted the glycolytic capacity. Besides, circMAGI3 overexpression promoted the proliferation. Therefore, these data suggested that circ-

MAGI3 could positively regulated the glycolysis and proliferation.

Up to now, the related research about circRNA and NSCLC has been achieved. For example, hsa_circ_0007385 is significantly upregulated in NSCLC tissue and cells, and hsa_circ_0007385 knockdown results in suppression of NSCLC cells' proliferation, migration and in-

vasion hsa_circ_0007385 knockdown, significantly reduced tumor growth. Bioinformatics inspires that hsa_circ_0007385 sponges a potential target miR-181, suggesting a possible regulatory pathway in NSCLC [9]. For another example, circFGFR1 is significantly upregulated in NSCLC and circFGFR1 over-expression is correlated with the unfavorable clinicopathological characteristics and poor prognoses. Cellular findings confirm that circFGFR1 directly interacts with miR-381-3p and subsequently act as a miRNA sponge to upregulate the target gene CXCR4 [18].

For the biological functions of circMAGI3, we found that circMAGI3 was mainly located in the cytoplasmic portion of NSCLC cells, suggesting the post-transcriptional regulation for circMAGI3. Online bioinformatics tools found that circMAGI3 functions as the sponge of miR-515-5p, thereby inhibiting the expression of miR-515-5p. In NSCLC, miR-515-5p has been reported as an anti-cancer gene. For example, Li J (2018) et al reported that miR-515-5p acts as a tumor suppressor by targeting CXCL6 in NSCLC cells and the low-expression of miR-515-5p is closely correlated with NSCLC survival and metastasis [19]. Therefore, circMAGI3 functions as an oncogene through inhibiting miR-515-5p. Then, we found that HDGF functions as a target for miR-515-5p. In human cancer, HDGF could accelerate the glycolysis of gastric cancer cells [20]. Overall, our findings revealed that circMAGI3/miR-515-5p/HDGF axis and its regulation on the glycolysis and proliferation of NSCLC cells.

In conclusion, this research illustrated the expression and biologic roles of circMAGI3 on the glycolysis and proliferation of NSCLC cells. Furthermore, this research also revealed the deepgoing mechanism of circMAGI3/miR-515-5p/HDGF axis, providing a vital theoretical basis for treatment of NSCLC.

Disclosure of conflict of interest

None.

Address correspondence to: Yushang Cui, Department of Thoracic Surgery, Peking Union Medical College Hospital, Peking Union Medical College and Chinese Academy of Medical Sciences, Beijing 100730, China. E-mail: cuiyushangdoctor@yeah.net

References

- [1] Hess LM, DeLozier AM, Natanegara F, Wang X, Soldatenkova V, Brnabic A, Able SL and Brown J. First-line treatment of patients with advanced or metastatic squamous non-small cell lung cancer: systematic review and network meta-analysis. *J Thorac Dis* 2018; 10: 6677-6694.
- [2] Houghton AM. Common mechanisms linking chronic obstructive pulmonary disease and lung cancer. *Ann Am Thorac Soc* 2018; 15: S273-s277.
- [3] Kabir TF, Chauhan A, Anthony L and Hildebrandt GC. Immune checkpoint inhibitors in pediatric solid tumors: status in 2018. *Ochsner J* 2018; 18: 370-376.
- [4] Kucharczuk CR, Ganetsky A and Vozniak JM. Drug-drug interactions, safety, and pharmacokinetics of egfr tyrosine kinase inhibitors for the treatment of non-small cell lung cancer. *J Adv Pract Oncol* 2018; 9: 189-200.
- [5] Pompili C, Absolom K, Franks K and Velikova G. Are quality of life outcomes comparable following stereotactic radiotherapy and minimally invasive surgery for stage I lung cancer patients? *J Thorac Dis* 2018; 10: 7055-7063.
- [6] Li X, Yang L and Chen LL. The biogenesis, functions, and challenges of circular RNAs. *Mol Cell* 2018; 71: 428-442.
- [7] Wu J, Qi X, Liu L, Hu X, Liu J, Yang J, Yang J, Lu L, Zhang Z, Ma S, Li H, Yun X, Sun T, Wang Y, Wang Z, Liu Z and Zhao W. Emerging epigenetic regulation of circular RNAs in human cancer. *Mol Ther Nucleic Acids* 2019; 16: 589-596.
- [8] Zhao W, Chu S and Jiao Y. Present scenario of circular RNAs (circRNAs) in plants. *Front Plant Sci* 2019; 10: 379.
- [9] Jiang MM, Mai ZT, Wan SZ, Chi YM, Zhang X, Sun BH and Di QG. Microarray profiles reveal that circular RNA hsa_circ_0007385 functions as an oncogene in non-small cell lung cancer tumorigenesis. *J Cancer Res Clin Oncol* 2018; 144: 667-674.
- [10] Jin M, Shi C, Yang C, Liu J and Huang G. Up-regulated circRNA ARHGAP10 predicts an unfavorable prognosis in NSCLC through regulation of the miR-150-5p/GLUT-1 axis. *Mol Ther Nucleic Acids* 2019; 18: 219-231.
- [11] Niu Y, Lin Z, Wan A, Chen H, Liang H, Sun L, Wang Y, Li X, Xiong XF, Wei B, Wu X and Wan G. RNA N6-methyladenosine demethylase FTO promotes breast tumor progression through inhibiting BNIP3. *Mol Cancer* 2019; 18: 46.
- [12] Wang S, Zhang Y, Cai Q, Ma M, Jin LY, Weng M, Zhou D, Tang Z, Wang JD and Quan Z. Circular RNA FDX1 promotes tumor progression and Warburg effect in gallbladder cancer by regu-

circMAGI3 accelerates the glycolysis of NSCLC

- lating PKLR expression. *Mol Cancer* 2019; 18: 145.
- [13] Wang Y, Liu J, Ma J, Sun T, Zhou Q, Wang W, Wang G, Wu P, Wang H, Jiang L, Yuan W, Sun Z and Ming L. Exosomal circRNAs: biogenesis, effect and application in human diseases. *Mol Cancer* 2019; 18: 116.
- [14] Wu N, Yuan Z, Du KY, Fang L, Lyu J, Zhang C, He A, Eshaghi E, Zeng K, Ma J, Du WW and Yang BB. Translation of yes-associated protein (YAP) was antagonized by its circular RNA via suppressing the assembly of the translation initiation machinery. *Cell Death Differ* 2019; 26: 2758-2773.
- [15] Zhou LY, Zhai M, Huang Y, Xu S, An T, Wang YH, Zhang RC, Liu CY, Dong YH, Wang M, Qian LL, Ponnusamy M, Zhang YH, Zhang J and Wang K. The circular RNA ACR attenuates myocardial ischemia/reperfusion injury by suppressing autophagy via modulation of the Pink1/FAM65B pathway. *Cell Death Differ* 2019; 26: 1299-1315.
- [16] Vilchez-Cavazos F, Millan-Alanis JM, Blazquez-Saldana J, Alvarez-Villalobos N, Pena-Martinez VM, Acosta-Olivo CA and Simental-Mendia M. Comparison of the clinical effectiveness of single versus multiple injections of platelet-rich plasma in the treatment of knee osteoarthritis: a systematic review and meta-analysis. *Pain Res Manag* 2019; 7: 232596711-9887116.
- [17] Li J, de Fraipont F, Gazzeri S, Cho WC and Eymen B. Circular RNAs and RNA splice variants as biomarkers for prognosis and therapeutic response in the liquid biopsies of lung cancer patients. *Front Genet* 2019; 10: 390.
- [18] Cheng M, Sheng L, Gao Q, Xiong Q, Zhang H, Wu M, Liang Y, Zhu F, Zhang Y, Zhang X, Yuan Q and Li Y. The m(6)A methyltransferase METTL3 promotes bladder cancer progression via AFF4/NF-kappaB/MYC signaling network. *Oncogene* 2019; 38: 3667-3680.
- [19] Li J, Tang Z, Wang H, Wu W, Zhou F, Ke H, Lu W, Zhang S, Zhang Y, Yang S, Ni S and Huang J. CXCL6 promotes non-small cell lung cancer cell survival and metastasis via down-regulation of miR-515-5p. *Biomed Pharmacother* 2018; 97: 1182-1188.
- [20] Wang Q, Chen C, Ding Q, Zhao Y, Wang Z, Chen J, Jiang Z, Zhang Y, Xu G, Zhang J, Zhou J, Sun B, Zou X and Wang S. METTL3-mediated m(6)A modification of HDGF mRNA promotes gastric cancer progression and has prognostic significance. *Gut* 2020; 69: 1193-1205.

circMAGI3 accelerates the glycolysis of NSCLC

Table S1. Sequences of shRNA and qRT-PCR primers

	5'-3'
circMAGI3	forward, 5'-CGACATCTGTCAGCAAGATGGA-3' reverse, 5'-CTTGCTGCAGTTTGTGGTCA-3'
sh-circMAGI3-1	5'-ACGCAGGCAAAGTCATTAATA-3'
sh-circMAGI3-2	5'-GGCAGTGGAAACGCAGGCAAA-3'
sh-circMAGI3-3	5'-GTGGAAACGCAGGCAAAGTCA-3'
miR-515-5p	forward, 5'-CGGGTTCTCCAAAAGAAAGCA-3' reverse, 5'-CAGCCACAAAAGAGCACAAT-3'
HDGF	forward, 5'-CTCTCCCTTACGAGGAATCCA-3' reverse, 5'-CCTTGACAGTAGGGTTGTTCTC-3'
U6	forward, 5'-CTCGCTTCGGCAGCACA-3' reverse, 5'-AACGCTTCACGAATTTGCGT-3'
beta-actin	forward, 5'-CTCCTTAATGTCACGCAGGATTC-3' reverse, 5'-GTGGGGCGCCCAGGCACCA-3'